RSC Advances

PAPER

View Article Online
View Journal | View Issue

Cite this: *RSC Adv.*, 2023, **13**, 9186

A universal green approach for the synthesis of NPS-codoped carbon quantum dots with enhanced broad-spectrum antibacterial and antioxidant activities†

Megha Pant,[a] Suresh Kumar,[a] Kumari Kiran,[a] Narendra Singh Bisht,[b] Veena Pande[a] and Anirban Dandapat *[c]

Bio-inspired quantum dots have received widespread attention in recent years due to their great potential for biological applications. Herein, we report a one pot hydrothermal synthesis of nitrogen–phosphorus–sulphur (NPS)-codoped carbon quantum dots from endophytic bacteria without using any additional doping precursor. The synthesized CQDs were thoroughly characterized and interestingly found to have a graphene like structure. The synthesized CQDs were then utilized in bactericidal activities against Gram-negative bacteria like *Salmonella typhi*, *Pseudomonas aeruginosa* and Gram-positive bacteria like the *Bacillus subtilis* strain. The strains were treated with different concentrations ranging from 5–100 μg ml^{-1}. The 5 μg ml^{-1} concentration appeared to be the MIC (minimum inhibitory concentration) and 100 μg ml^{-1} is the MBC (minimum bactericidal concentration) maintaining a short incubation period of one hour. A simple, cost-effective and eco-friendly approach to synthesize multi-elemental doped CQDs would certainly cause the method to be used in future for diverse biological applications. As compared to the broadly used antibiotics, the developed CQDs have some added advantages including lower cytotoxicity, excellent photo-stability and high selectivity.

Received 19th December 2022
Accepted 5th March 2023

DOI: 10.1039/d2ra08103b

rsc.li/rsc-advances

1 Introduction

Since their discovery in 2004, carbon quantum dots (CQDs) have been widely utilized in various fields owing to their very attractive properties, *e.g.* chemical inertness, high water solubility, low toxicity, ease of functionalization and photostability.[1–3] At present, CQDs are utilized in every possible field including catalysis, sensing, bio-imaging, optoelectronic devices, energy storage devices, drug and gene delivery, bactericidal agents, *etc.*[4–6] In contrast to conventional metal/semiconductor quantum dots, CQDs have less toxicity and higher biocompatibility, which make them an ideal material to be utilized in biomedical fields.[7,8] Studies have shown that heteroatom doping can significantly improve the properties of CDs. In this area, currently, extensive research is going on to establish easy and economic methods to synthesize heteroatom-doped CQDs. Heteroatoms (*e.g.* N, P, S *etc.*) with different size and electronegativities than carbon create defects in the crystal structure of CQDs and thus introduce high density of active sites, which will make them suitable for various applications.[9,10] In addition, N, S and P co-doping may also provide better carrier separation for enhanced activities. Therefore, defects mediated reactive oxygen species and enhanced charge separation will make NPS-doped-CQDs an ideal candidate for bactericidal activities.[11]

In literature, mainly chemical methods have given to synthesize doped-CQDs utilizing the heteroatom containing compounds as precursor.[12] However, biosynthesis of any nanoparticles has been proposed as the cost-effective and environmentally friendly alternative to chemical and physical methods.[13,14] Bio-synthesized nanoparticles are highly recommended especially for biological applications. Recently, different biological precursors containing different heteroatoms (mainly N, P and S) are used to fabricate doped-CQDs.[15] Wang *et al.* used cucumber juice to synthesize NPS co-doped CQDs by hydrothermal method.[16] However, for large-scale synthesis, plant source-mediated synthesis is not encouraging for environmental imbalance. In this perspective, use of bacteria, which are easy to grow on laboratory on mass scale, could be an alternate option to use as carbon precursor in CQDS. Very recently, Zhang *et al.* used bacteria isolated from the industrial sewage of a Kunming steel

[a]*Department of Biotechnology, Sir J. C. Bose Technical Campus, Bhimtal, Kumaun University, Nainital, Uttarakhand - 263136, India*

[b]*Department of Chemistry, DSB Campus, Kumaun University, Nainital, Uttarakhand - 263002, India*

[c]*University School of Automation and Robotics, Guru Gobind Singh Indraprastha University, East Delhi Campus, Surajmal Vihar, Delhi-110092, India. E-mail: dranirbandandapat@kunainital.ac.in*

† Electronic supplementary information (ESI) available. See DOI: https://doi.org/10.1039/d2ra08103b

factory to synthesize CQDs.[17] Again, although CQDs itself is non-hazardous, their precursors are not always safe. Therefore, use of endophytic bacteria as carbon precursors could be the best alternate option, which is yet to be explored.[18]

Microbial contaminations are one of the major threat to public health throughout the world. Microorganisms now have developed various tactics to bypass the antimicrobial compounds. Major concern in this area is the multidrug resistance (MDR) developed by the microorganism against the antibiotic drugs.[19] With the advancement in technology, currently, different nanomaterials are used to replace the conventional antibiotics and fight with the problem of MDRs. However, majority of the materials possess threats related to environmental hazards, poor biocompatibility and high cost. Therefore, cheap, durable, sustainable and effective antimicrobial agents for long-term applications are in high demand. In this context, utilization of CQDs could provide an effective solution. Due to their small size CQDs interact with the bacterial species making them an excellent nanomaterial to be used for bactericidal properties.[20,21] Maintaining the cell membrane integrity is one of the crucial factors required for the survival of bacteria. The main mechanism behind the bactericidal activity of the carbon quantum dots is related to their ability to disrupt the cell-membrane integrity.[22–24] Even though, there are few reports on the utilization of CQDs for antibacterial activities, most of them exhibit their activities at acidic pH but have poor activity under physiological conditions of around neutral pH.

Current work has established a general green method for the synthesis of NPS co-doped CQDs which are highly active under neutral pH. We have isolated endophytic bacteria from the plant *urtica dioica* and used as the starting precursor material for the synthesis of CQDs *via* one pot hydrothermal synthesis method. The *urtica dioica* is a commonly available plant and known to have different therapeutic and medicinal properties. Among the isolated endophytic bacteria, *Bacillus megatarium* known to be an important industrial bacterium since ages was further used. Bacteria-derived CQDs displays excellent antimicrobial activities against all the tested pathogenic strains *viz. Salmonella typhi, Pseudomonas aeruginosa* and *Bacillus subtilis* at neutral pH. To the best of our knowledge, this is the first report of any endophytic bacteria-derived indigenous NPS co-doped CQDs which are synthesised in one-step process without any foreign doping precursors.

2 Experimental

2.1 Chemicals for isolation of endophytic bacteria and synthesis of CQDs

Tween 20, sodium hypochlorite, ethanol, hydrogen peroxide and mercuric chloride was purchased from Sisco Research Laboratories Pvt. Ltd. Dialysis membrane MWCO of >1 kDa. was obtained from Sigma-Aldrich.

2.2 Chemicals for antibacterial assay

Luria-Bertani broth and agar powders were obtained from Hi-Media Laboratories. The Gram-negative and Gram-positive bacterial strains MTCC 3224, MTCC 424 and MTCC 441 were purchased from MTCC Chandigarh, India.

2.3 Isolation of endophytic bacteria

The leaf and stem samples of *Urtica dioica* L. were collected using a sterile scalpel from DBT campus, Bhimtal, K. U. Uttarakhand. The samples were kept in sterile plastic bags and were used within 24 hours for further studies. To remove the surface epiphytes, the samples were thoroughly washed followed by washing in Tween 20 for 1 minute in laminar air flow. It is then given treatment of 1–5% sodium hypochlorite for 2–10 minutes then Ethanol 70–95% for 30 seconds finally 0.2% hydrogen peroxide and mercuric chloride for 2–5 minutes. In laminar air flow after proper drying of the sample the surface of the stem was removed and the leaves were cut into small pieces and placed on N. A. medium on the sterile plates. The plates were then incubated at 37 °C for 24 hours.[25] The colonies obtained were differentiated on the basis of morphology. Single colonies were picked from plates and streaked to obtain pure bacterial colonies. The inoculation process repeated till monocultures were obtained for further experimentation.

2.4 Synthesis of CQDs

CQDs were prepared through one pot hydrothermal carbonization of B-1 bacterial strain. The isolated bacterial strain was grown overnight with shaking in L. B. broth. The culture was then centrifuged (10 000 g, 15 min, 4 °C). The cells were finally washed with double distilled water for at-least three times to remove the supernatant. The pellet obtained was then re-suspended in 30 ml of distilled water (30 ml). Subsequently, the bacterial suspension was transferred into a Teflon-lined stainless-steel autoclave and heated up to 200 °C for 24 hours. A light brownish solution was obtained. The obtained solution was then filtered through a syringe filter (0.22 μm) diameter to remove large particles. Finally, after dialyzing using dialysis membrane of (MWCO > 1 kDa) against deionized water for 72 hours, the CQD solution was obtained and stored at 4 °C for further experiments.[26] Repeatability was further checked by repeating the same experiment thrice.

2.5 Quantum yield measurement

The quantum yield (QY) was determined using the standard procedure[27] with quinine sulphate in 0.1 M H_2SO_4 as a reference (QY = 54 percent excited at 338 nm = 1.33). The following equation can be used to calculate QY:

$$Q_{CQDs} = Q_R(I_{CQDs}/I_R)\ (A_R/A_{CQDs})(\eta_{CQDs}{}^2/\eta_R{}^2)$$

where Q_{CQDs} is the quantum yield of the as-prepared CQDs, I is the integrated emission intensity, η is the refractive index of the solvent utilized, and A is the absorbance at the excitation wavelength. The abbreviations CQDs and R stand for "prepared CQDs" and "reference," respectively.

2.6 Characterization of endophytic bacteria

The endophytic bacterial strain was identified *via* molecular identification. The kit obtained from Hi-media was used to isolate genomic DNA. To identify the strain, PCR amplification of extracted DNA with 16S universal primers was used. After completion of PCR, the PCR results were verified on a 1% agarose gel electrophoresis using the reference ladder and observed under UV light by using ethidium bromide. By comparing the PCR product to a ladder, the DNA product was identified. To investigate phylogenetic relationships, the isolate's 16s sequences were matched with sequencing data of bacterial strains which are taxonomically identical (retrieved from the NCBI) and a phylogram was created using the MEGA X software. To obtain the more accurate evolutionary history of our sequence we performed bootstrap to create 1000 replicas of the phylogenetic tree generated using neighbor joining method.

2.7 Characterization of CQDs

Size determination of CQDs were determined by using a Transmission Electron Microscope (JEM-2100F, 200 kV, JEOL, Fresing, Germany). The average size diameter was calculated using image J software. Fluorescence spectra were recorded on the LS 55 (PerkinElmer) fluorescence spectrophotometer with excitation range of 200–800 nm. UV-vis spectra from were obtained by Thermo Scientific Evolution 260 B10. FT-IR analysis was recorded using PerkinElmer Spectrum 2 using ATR method. X-ray Photoelectron Spectrum (XPS) was obtained using ESCA+, (omicron nanotechnology, Oxford Instrument Germany) outfitted with a monochromator aluminium source (Al Kα radiation, $\hbar\nu = 1486.7$ eV).

2.8 Antibacterial assay

Using the standard colony forming unit (CFU) counting method antibacterial assay was performed. Overnight grown cultures of Gram-negative bacteria *Salmonella typhi*, *Pseudomonas aeruginosa* and Gram-positive bacteria *Bacillus subtilis* were used. These cultures were grown in L. B. broth at 37 °C for 24 h with shaking at 150 rpm. The cultures were then diluted with a dilution factor of 10^{-7}. Different concentration of CQDs starting from 5 μg ml^{-1}, 25 μg ml^{-1}, 50 μg ml^{-1} and 100 μg ml^{-1} was taken and incubated at 37 °C for 1 hour with the diluted bacterial culture. After an hour interval the subsequent bacterial culture with CQDs were plated on L. B agar plates and incubated overnight at 37 °C. The experiment was performed in triplicates. Percentage survival rate was calculated using the following equation.

$$\%\ \text{survival rate} = [((\text{number of colonies})_{\text{control}} - (\text{number of colonies})_{\text{sample}})/(\text{number of colonies})_{\text{control}}] \times 100$$

2.9 DPPH assay for antioxidant evaluation

DPPH assay was done to evaluate the antioxidant potential of the synthesized CQDs. DPPH (1,1-diphenylpicrylhydrazyl) over the course of time it changes its color from deep violet to colorless in the presence of antioxidants. The assay was performed using the biosynthesized CQDs using Ruiz *et al.* (2017) method with some modifications.[28] For the assay different concentrations (10, 20, 30, 40, 50 and 60 μg ml^{-1}) of CQDs was taken. 1 ml of methanolic DPPH (4 mg/100 ml) was mixed with 1 ml of different methanolic concentrations. The samples were then loaded onto the wells of 96 micro-titer plate and the plate was kept in dark for 30 minutes. The absorbance was recorded at 517 nm in Elisa plate reader. Ascorbic acid (1 mg ml^{-1}) as positive and methanol as negative control was taken. The experiments were done in triplicates. The percentage scavenging activity was calculated as:

$$\%\ \text{scavenging activity} = [(A_{\text{control}} - A_{\text{sample}})/(A_{\text{control}})] \times 100$$

where A is the absorbance.

3 ABTS radical scavenging activity

ABTS 2,2′-azino-bis (3- ethylbenzothiazoline-6-sulphonic acid) assay is the widely used assay to determine the antioxidant potential of the compound. The assay is mainly based on quenching of ABTS$^{\bullet}$ radical. The antioxidant capacity was determined according to Re *et al.* (1999) with slight modifications.[29] A 7 mM ABTS stock solution was prepared. The solution was then reacted with a stock solution of 2.45 mM potassium persulfate to generate the ABTS radical cation (ABTS+). Before use the final solution was kept in dark for 12–16 h and the absorbance of solution was adjusted to 0.70 O. D value at 734 nm. Different concentration of CQDs were then treated with ABTS to a final concentration of 3 ml. The samples were then incubated for 6 min after which the absorbance was determined at 734 nm. The percentage inhibition was calculated by:

$$\%\ \text{inhibition activity} = [(A_{\text{control}} - A_{\text{sample}})/(A_{\text{control}})] \times 100$$

4 Results and discussion

The nucleotide sequence was submitted in the Genbank (Accession No. OK303397). The phylogenetic analysis of 16S DNA sequence of the isolated bacterial culture was obtained using the neighbour-joining method which determines the branch length as well as topology of the phylogenetic tree. The results show 100% similarity with *Bacillus megaterium* strain of our identified bacterial strain of *Bacillus megaterium* (Fig. 1). Subsequently the isolated endophytic bacteria were used as precursor for hydrothermal synthesis of doped CQDs.

One of the fascinating feature of C-dots is its optical properties. The optical image of CQDs displays brown colour under normal light, whereas it shows bluish-green luminescence under UV light of wavelength 365 nm (inset of Fig. 2a). UV-visible absorption spectrum (Fig. 2a) shows peaks at ~270 nm and a broad shoulder at ~330 nm. The former peak arrives due to the π–π* transitions of sp^2 carbon atoms, representing the

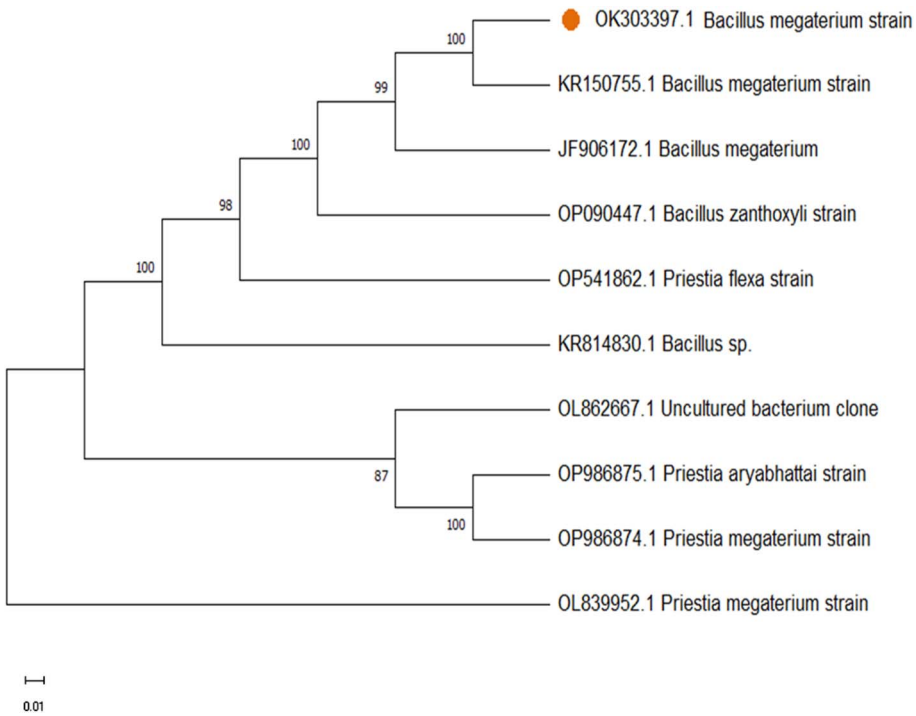

Fig. 1 Phylogenetic tree of the endophytic bacterial isolate identified as *Bacillus megaterium* strain.

formation of graphitized carbon particles.[30] The later peak refers to the n–π* transition mainly due to the presence of different functional groups (especially C=O).[31] Upon excitation (wavelength ranges of ~340–480 nm) it shows broad and strong emission peaks as shown in Fig. 2b. Highest intensity peak observed at 420 nm upon excitation with 360 nm is the effect of

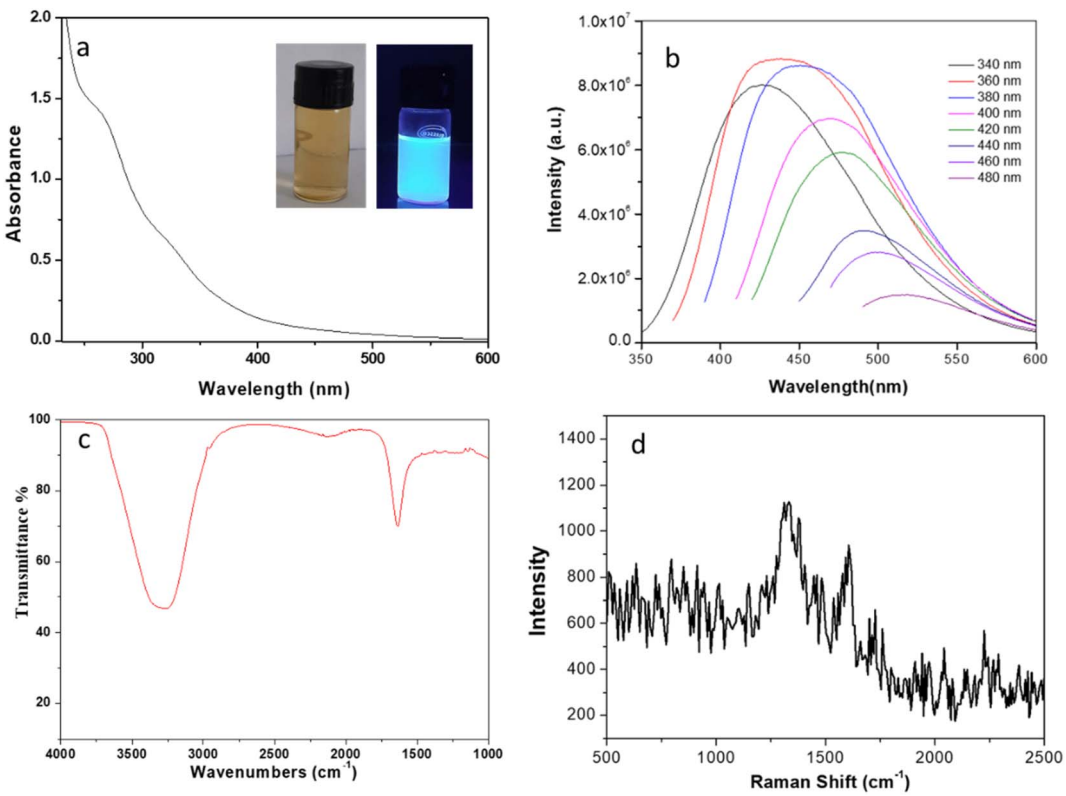

Fig. 2 (a) UV-vis absorption spectra of CQDs; inset shows the photograph under visible light and UV light (365 nm) irradiation. (b) Fluorescence spectra of CQDs under different wavelengths (340–480 nm) (c) FTIR spectrum of as synthesized CQDs (d) Raman spectra of CQDs.

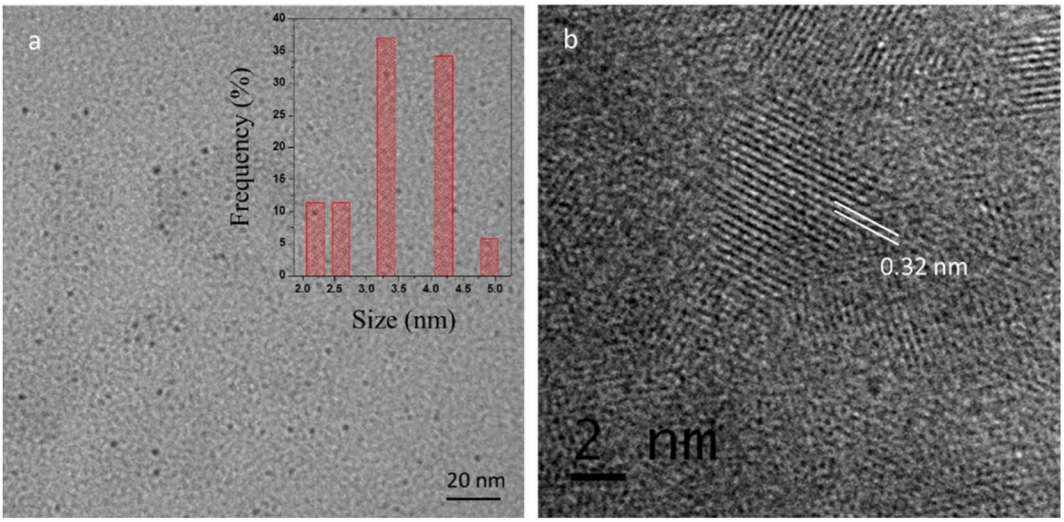

Fig. 3 (a) TEM image of CQDs (inset shows the particle size distribution of corresponding CQDs) (b) HRTEM image of CQDs showing the lattice fringes.

different surface states of C-dots.[32] The excitation-dependent spectra show a shift in photoluminescence (PL) peak from 420 to 520 nm under excitation range of 340–480 nm as shown in Fig. 2b. Several hypotheses have been proposed to explain the wavelength – dependent emission spectra of CQDs.[33] As the carbon particle decreases in size, quantum confinement takes place meaning that the particle is smaller than the de Broglie wavelength of the electron in the dot, creating a deviation from bulk properties. This confinement creates a quantization of the energy into discrete levels in the conduction and valence bands, so the C-dot can be understood as "virtual atom". The emission energy depends on the radius of the particle so that as the particle gets smaller, both the excitation and emission spectra shift to shorter wavelengths. In a distribution of C-dots with varying sizes, different subsets get preferentially excited as the excitation wavelength varies. As CQDs of different size are excited, the emission spectrum shifts with excitation wavelength.[34] Another potential explanation for the PL behaviour of carbon dots is the existence of different emissive sites on the surface of the dot. These sites are related to different defects on the surface, which are selectively excited depending on the wavelength used. With quinine sulphate as the reference, the quantum yield of the synthesized CQDs was measured to be ~30% under the excitation of 360 nm, which is a relatively high degree in comparison to the previous literature and proves the material's capability in fluorescence based sensing and bio-imaging applications. FTIR spectrum of the synthesized CQDs was analysed to determine their surface functional groups. The very broad peak at 3307 cm^{-1} is attributed to the asymmetric stretching vibrations of –OH and/or N–H groups. Another weak band at 2131 cm^{-1} may be attributed to C–N vibration.[35] One of the intense characteristic peak at 1639 cm^{-1} assigned to aromatic C=C stretching vibrations.[36] The Raman spectra for the synthesized CQDs as seen in Fig. 2d shows the characteristic G band at 1615 cm^{-1} and D band at 1330 cm^{-1} with an intensity ratio I_D/I_G ~1.2.[37] XRD pattern (ESI, Fig. S1†) of the developed materials shows a broad peak appeared at ~23°, which can be indexed to the (002) crystal plane of graphene QDs. Therefore, characterization of the synthesized carbon quantum dots supports the formation of graphene like structure.

The dispersion of the CQDs was verified by the TEM (Transmission electron microscopy) as shown in Fig. 3a. The TEM image revealed that the synthesized CQDs have a narrow size distribution of ~2–5 nm (average size 3.5 ± 0.4 nm). High-resolution TEM image (Fig. 3b) shows the lattice fringes of 0.32 nm corresponding to (002) plane of graphene[38] which reveal that CQDs display typical to graphitic carbon lattice parameters.

Elemental composition and speciation within the developed CQDs were determined by XPS. The XPS survey scan spectrum as shown in Fig. 4a indicates the presence of intense peaks at ~284.6 eV, ~399.0 eV, ~531.0 eV, ~133.1 eV and ~169.6 eV attributed to characteristic peaks of carbon (C 1s), nitrogen (N 1s), oxygen (O 1s), phosphorous (P 2p) and sulphur (S 2p), respectively. Fig. 4b–f describes the high-resolution short scanned XPS spectra of C 1s, N 1s, O 1s, P 2p and S 2p, respectively. The three fitted peaks in the high-resolution C 1s attributed to sp^2 graphitic carbon, carbonyl and carboxylic groups, as depicted in the figure. The N 1s peaks indicate the existence of nitrogen-containing groups, C–N–C and N–H, at 399.4 and 401.1 eV, respectively, which are assigned to amides and/or amino groups. The oxygen element in the forms of C=O and C–O, respectively, are assigned to the two fitted peaks at 531.6 and 532 eV in the O 1s spectra.[39,40] The peaks of P 2p at 132.8 eV and 133.7 eV can be assigned to P–O and P=O bonds, respectively. For S 2p spectra, the contribution at 167.6 eV can be assigned to sulfonic acids, and the peak at 168.8 eV is assigned to sulphate groups.[41] This conforms the doping of N, P, S within the network of graphene like carbon dots during the synthesis. The contents of C, O, N, P, and S were ~50.48%, 35.09%, 9.93% 0.96 and 3.35% respectively. The total doping content (especially nitrogen) was higher as compared to

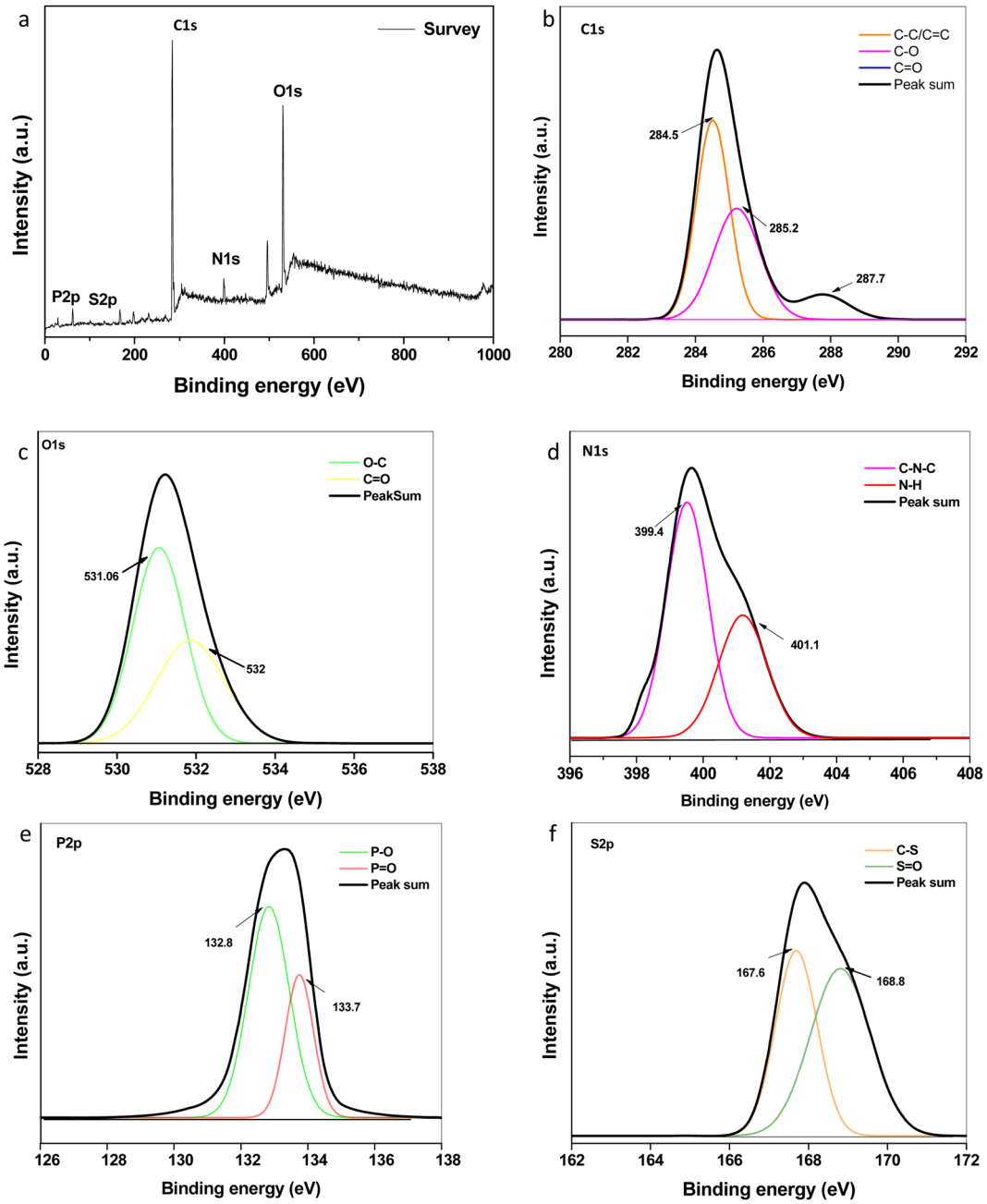

Fig. 4 High-resolution XPS spectrum: (a) survey scan (b) C 1s (c) O 1s (d) N 1s (e) P 2p and (f) S 2p spectra of the synthesized CQDs.

previous reports of CQDs synthesized using different plant sources.[42–44] The synergic effect of doping, composition, and functional groups could be their utility in various fields. Herein, we checked the antimicrobial and antioxidant activities of the developed CQDs.

Antibacterial activities of the developed CQDs was investigated against both Gram-positive and Gram-negative bacteria *viz. Salmonella typhi*, *Pseudomonas aeruginosa* and *Bacillus subtilis*. As shown in Fig. 5, different concentrations (5–100 μg ml^{-1}) of CQDs were used and the number of viable colonies were found to be significantly decreased with increasing the concentration of CQDs. Upon reaching the highest concentration *i.e.* 100 μg ml^{-1} no bacterial colonial growth was observed on the L. B. agar plates against *Salmonella typhi* and *Pseudomonas aeruginosa*. Whereas, 75 μg ml^{-1} of CQDs was sufficient for 100% inhibition of bacterial growth against the *Bacillus subtilis*.

The minimum inhibitory concentration (MIC) and minimum bactericidal concentration (MBC) was also determined. MIC of CQDs against *Salmonella typhi*, *Pseudomonas aeruginosa* and *Bacillus subtilis* was calculated to be around 5 μg ml^{-1}. The antibacterial properties of CQDs are mainly influenced by their extremely small size and surface functional groups. In a study[45] it was seen that the role of surface charges presents on CQDs plays a crucial role in interacting with the bacterial cell wall thus also helping in the labelling of the

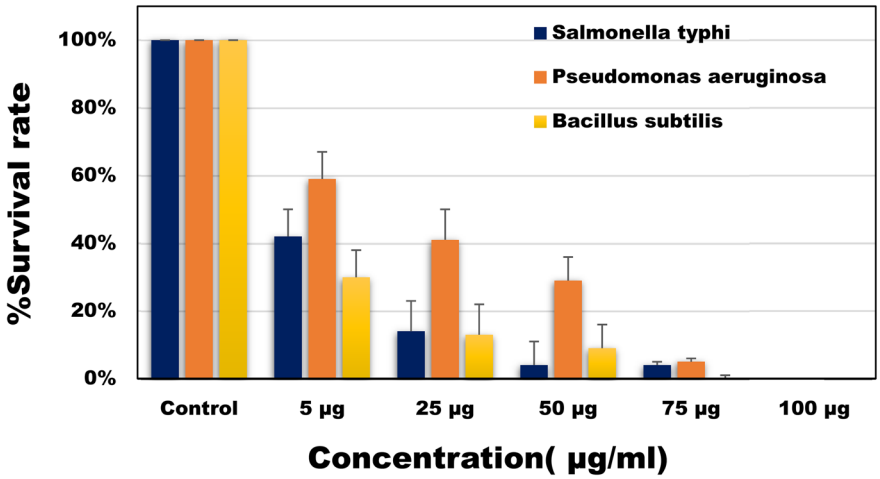

Fig. 5 Percentage survival rate of the bacterial species (*Salmonella typhi*, *Pseudomonas aeruginosa* and *Bacillus subtilis*) against different concentrations of CQDs.

bacterial cells.[46] The bactericidal property of CQDs can be described as the destruction of the bacterial membrane (ESI; Fig. S2†), leaking of cytoplasmic material thus finally resulting in cell apoptosis.[47] Comparative studies showed that the superior activities of developed CQDs as compared to most of the previously reported CQDs (Table 1).

4.1 Radical scavenging (DPPH) assay

The non-toxic nature of CQDs made them exceptional materials suitable for different biological applications. Antioxidant capacity of the synthesized CQDs was analysed using the well-established DPPH assay.[56] The bacterial derived CQDs showed excellent free radical scavenging activity. This rise in scavenging property can be attributed to the different functional groups carboxyl, hydroxyl and amide groups present on the surface of the CQDs. At concentration of 60 μg ml^{-1}, it shows the highest scavenging activity (~75%) (Fig. 6). The EC50 of the CQDs was calculated to be around 24.78 μg ml^{-1} as compared to the EC50 of the standard ascorbic acid of 5.36 μg ml^{-1}. Compared to previous reports of CQDs (ESI; Table S1†), the present material

Table 1 Comparative study of antibacterial activity of different CQDs synthesized from natural precursors

Materials	Size	Method of synthesis	MIC values	Strain	References
Cu doped NCQDs	7.2 nm	Hydrothermal	600 μg ml^{-1}	*E. coli* *S. epidermidis*	48
Ag@S-GQDs nanocomposite	4.0 nm	Pyrolysis	70 μg ml 35 μg ml	*P. aeruginosa* *S. aureus*	49
Sugarcane pulp derived CQDs	2.27 nm	Hydrothermal	—	*Benthesicymus cereus* *S. aureus* *Pseudomonas aeruginosa* *Vibrio cholera* *E. coli*	50
Pomegranate (P-Cdots) and watermelon peels (WC-dots) derived CDs	5.0 nm	Microwave	40 μg ml^{-1}	*Pseudomonas aeruginosa* *Bacillus Subtilis* *S. aureus*	51
NSP-CQDs	4.0–5.0 nm	Microwave	100 μg ml^{-1}	*E. coli* *S. aureus*	52
P-doped CQDs	3.4 nm	Hydrothermal	1.23 mg ml^{-1} 1.44 mg ml^{-1}	*E. coli* *S. aureus*	53
Curcuma longa derived CDs	2.6 nm	Hydrothermal	0.25 mg ml^{-1} 0.5 mg ml^{-1}	*E. coli* *S. aureus* *K. pneumoniae* *S. epidermidis*	54
Mushroom-derived CDs	8.0 nm	Hydrothermal	30.0 μg ml^{-1}	*S. aureus* *K. pneumoniae* *Pseudomonas aeruginosa*	55
Endophytic bacteria derived CDs	3.5 nm	Hydrothermal	5.0 μg ml^{-1}	*Salmonella typhi* *Pseudomonas aeruginosa* *Bacillus subtilis*	Present work

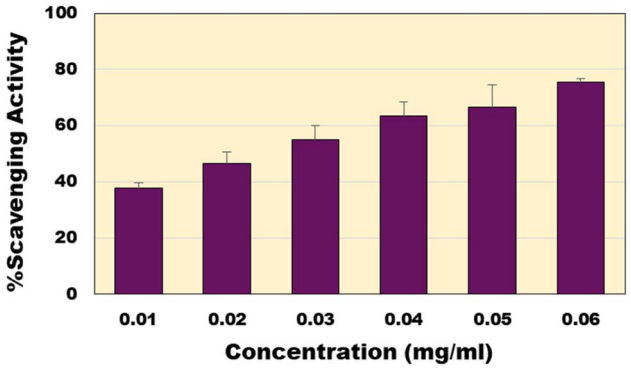

Fig. 6 Percentage scavenging activity of CQDs at various concentrations.

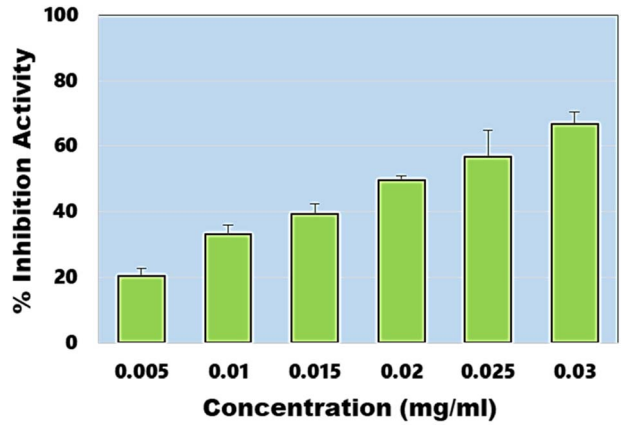

Fig. 7 Percentage inhibition activity of synthesized CQDs calculated against different concentration ranges.

shows much higher activity except a recent report where similar activities were reported.[57]

4.2 ABTS assay

In addition to DPPH assay, ABTS assay also known as Trilox equivalent antioxidant-capacity assay was also performed. The assay provides an easy, rapid and more sensitive means to evaluate antioxidant potential of any material. In this assay, EC50 value was estimated to be ~20.65 μg ml^{-1} (Fig. 7), which is close to the EC50 value obtained during DPPH assay. Under similar conditions, EC50 of the ascorbic acid was estimated to be ~4.27 μg ml^{-1}. These results confirm the synthesis of highly efficient graphene-like carbon quantum dots which have shown very high antimicrobial and antioxidant activities.

5 Conclusion

Present study describes an easy and facile approach for the synthesis of NPS co-doped CQDs from endophytic bacteria without using any other chemicals for doping. The synthesized CQDs have mainly graphene-like structure. They possess exceptional antioxidant and broad spectrum of bactericidal activities due to their tiny size (~3 nm) and surface functional groups. The small size of the CQDs help them to penetrate the bacterial membrane and thus helps in reactive oxygen species generation thus leading to cell apoptosis. This material does not require any further doping or functionalization as it was abundant source of carbon, nitrogen, sulphur and oxygen. Moreover, our approach can further broaden the use of endophytic bacteria in more biological applications.

Conflicts of interest

There are no conflicts to declare.

Acknowledgements

The authors would like to express deep gratitude for the support of DST, Govt. of India for financial assistance through the INSPIRE Faculty Award (IFA16-MS81). Authors wish to express sincere gratitude to the administration of GGSIP University for providing the academic environment to pursue research activities.

References

1 X. Chen, Z. Song, S. Li, N. T. Thang, X. Gao, X. Gonga and M. Guo, *Green Chem.*, 2020, **22**, 3296–3308.
2 C. He, X. Li, G. Fenga and W. Long, *Green Chem.*, 2014, **16**, 2566–2570.
3 M. Shamsipur, A. Barati and S. Karami, *Carbon*, 2017, **124**, 429–472.
4 B. Geng, Y. Li, J. Hu, Y. Chen, J. Huang, L. Shen, D. Pan and P. Li, *J. Mater. Chem. B*, 2022, **10**, 3357–3365.
5 M. L. Liu, B. B. Chen, C. M. Li and C. Z. Huang, *Green Chem.*, 2019, **21**, 449–471.
6 Z. X. Liu, B. B. Chen, M. L. Liu, H. Y. Zou and C. Z. Huang, *Green Chem.*, 2017, **19**, 1494–1498.
7 B. Geng, J. Hu, Y. Li, S. Feng, D. Pan, L. Feng and L. Shen, *Nat. Commun.*, 2022, **13**, 5735.
8 B. Geng, S. Xu, P. Li, X. Li, F. Fang, D. Pan and L. Shen, *Small*, 2022, **18**, 2103528.
9 S. Miao, K. Liang, J. Zhu, B. Yang, D. Zhao and B. Kong, *Nano Today*, 2020, **33**, 100879.
10 F. Li, D. Yang and H. Xu, *Chem. – Eur. J.*, 2019, **25**, 1165–1176.
11 X. Gon, Y. Liu, Z. Yang, S. Shuang, Z. Zhang and C. Dong, *Anal. Chim. Acta*, 2017, **968**, 85–96.
12 M. Zan, L. Rao, H. Huang, W. Xie, D. Zhu, L. Li, X. Qie, S. S. Guo, X. Z. Zhao, W. Liu and W. F. Dong, *Sens. Actuators, B*, 2018, **262**, 555–561.
13 C. He, X. Li, G. Fenga and W. Long, *Green Chem.*, 2022, **24**, 5842–5855.
14 S. Chahal, J. Macairan, R. Yousefi, N. Tufenkji and R. Naccache, *RSC Adv.*, 2021, **11**, 25354–25363.
15 X. Kou, S. Jiang, S. J. Park and L. Y. Meng, *Dalton Trans.*, 2020, **49**, 6915–6938.
16 C. Wang, D. Sun, K. Zhuo, H. Zhang and J. Wang, *RSC Adv.*, 2014, **4**, 54060–54065.

17 S. Zhang, D. Zhang, Y. Ding, J. Hua, B. Tang, X. Ji, Q. Zhang, Y. Wei, K. Qin and B. Li, *Analyst*, 2019, **144**, 5497–5503.
18 A. Kumar, S. Kumar, K. Kiran, S. Banerjee, V. Pande and A. Dandapat, *Colloids Surf., B*, 2021, **206**, 111948.
19 F. Prestinaci, P. Pezzotti and A. Pantosti, *Pathog. Global Health*, 2015, **109**, 309–318.
20 M. Alavi, E. Jabari and E. Jabbari, *Expert Rev. Anti-Infect. Ther.*, 2021, **19**, 35–44.
21 Y. Sun, M. Zhang, B. Bhandari and C. Yang, *Food Rev. Int.*, 2020, **7**, 1–20.
22 N. S. Bisht, A. H Tripathi, M. Pant, S. K. Upadhyay, N. G. Sahoo, S. P. S. Mehta and A. Dandapat, *Colloids Surf., B*, 2022, **217**, 112640.
23 H. Wang, Z. Song, J. Gu, S. Li, Y. Wu and H. Han, *ACS Biomater. Sci. Eng.*, 2019, **5**, 4739–4749.
24 D. Pancholi, N. S. Bisht, V. Pande and A. Dandapat, *Colloids Surf., B*, 2021, **199**, 111558.
25 N. Anjum and R. Chandra, *Asian J. Pharm. Clin. Res.*, 2015, **8**, 233–238.
26 F. Lin, C. Li and Z. Chen, *Front. Microbiol.*, 2018, **9**, 259.
27 C. Zhao, Y. Jiao, J. Hua, J. Yang and Y. Yang, *J. Fluoresc.*, 2018, **28**, 269–276.
28 V. Ruiz, L. Yate, I. García, G. Cabanero and H. J. Grande, *Carbon*, 2017, **116**, 366–374.
29 R. Re, N. Pellegrini, A. Proteggente, A. Pannala, M. Yang and C. Rice-Evans, *Free Radical Biol. Med.*, 1999, **26**, 1231–1237.
30 Y. Li, H. Shu, X. Niu and J. Wang, *J. Phys. Chem. C*, 2015, **119**, 24950–24957.
31 S. Zhang, D. Zhang, Y. Ding, J. Hua, B. Tang, X. Ji and B. Li, *Analyst*, 2019, **144**, 5497–5503.
32 Y. S. Lin, Y. Lin, A. P. Periasamy, J. Cang and H. T. Chang, *Nanoscale Adv.*, 2019, **1**, 2553–2561.
33 L. Guo, J. Ge, W. Liu, G. Niu, Q. Jia, H. Wang and P. Wang, *Nanoscale*, 2016, **8**, 729–734.
34 S. Zhu, Y. Song, X. Zhao, J. Shao, J. Zhang and B. Yang, *Nano Res.*, 2015, **8**, 355–381.
35 M. Shariati-Rad, T. Mohseninasab and F. Parno, *RSC Adv.*, 2018, **8**, 2173–2180.
36 W. Yang, J. Ni, F. Luo, W. Weng, Q. W. Z. Lin and G. Chen, *Anal. Chem.*, 2017, **89**, 8384–8390.
37 Y. Fang, S. Guo, D. Li, C. Zhu, W. Ren, S. Dong and E. Wang, *ACS Nano*, 2012, **6**, 400–409.
38 J. Kim and J. S. Suh, *ACS Nano*, 2014, **8**, 4190–4196.
39 F. Yan, Z. Bai, F. Zu, Y. Zhang, X. Sun, T. Ma and L. Chen, *Microchim. Acta*, 2019, **186**, 1–11.
40 X. W. Hua, Y. W. Bao, H. Y. Wang, Z. Chen and F. G. Wu, *Nanoscale*, 2017, **9**, 2150–2161.
41 N. A. Travlou, D. A. Giannakoudakis, M. Algarra, A. M. Labella, E. Rodríguez-Castellón and T. J. Bandosz, *Carbon*, 2018, **135**, 104–111.
42 J. Zhong, X. Chen, M. Zhang, C. Xiao, L. Cai, W. A. Khan, K. Yu, J. Cui and L. He, *Chin. Chem. Lett.*, 2020, **31**, 769–773.
43 H. Wang, M. Zhang, Y. Ma, B. Wang, M. Shao, H. Huang, Y. Liu and Z. Kang, *J. Mater. Chem. B*, 2020, **8**, 2666–2672.
44 C. Wang, D. Sun, K. Zhuo, H. Zhang and J. Wang, *RSC Adv.*, 2014, **4**, 54060–54065.
45 M. Gagic, S. Kociova, K. Smerkova, H. Michalkova, M. Setka, P. Svec and V. Milosavljevic, *J. Colloid Interface Sci.*, 2020, **580**, 30–48.
46 C. I. Weng, H. T. Chang, C. H. Lin, Y. W. Shen, B. Unnikrishnan, Y. J. Li and C. C. Huang, *Biosens. Bioelectron.*, 2015, **68**, 1–6.
47 M. A. Quinteros, C. A. Viviana, R. Onnainty, V. S. Mary, M. G. Theumer, G. E. Granero and P. L. Páez, *Int. J. Biochem. Cell Biol.*, 2018, **104**, 87–93.
48 F. Nichols, J. E. Lu, R. Mercado, M. D. Rojas-Andrade, S. Ning, Z. Azhar and S. Chen, *Langmuir*, 2020, **36**, 11629–11636.
49 S. Kadian, G. Manik, N. Das, P. Nehra, R. P. Chauhan and P. Roy, *J. Mater. Chem. B*, 2020, **8**, 3028–3037.
50 S. Pandiyan, L. Arumugam, S. P. Srirengan, R. Pitchan, P. Sevugan, K. Kannan and V. Gandhirajan, *ACS Omega*, 2020, **5**, 30363–30372.
51 W. A. Qureshi, B. Vivekanandan, J. A. Jayaprasath, D. Ali, S. Alarifi and K. Deshmukh, *J. Nanomater.*, 2021, **2021**, 9096838.
52 K. M. Tripathi, H. T. Ahn, M. Chung, X. A. Le, D. Saini, A. Bhati and T. Kim, *ACS Biomater. Sci. Eng.*, 2020, **6**, 5527–5537.
53 S. Chai, L. Zhou, S. Pei, Z. Zhu and B. Chen, *Micromachines*, 2021, **12**, 1116.
54 A. Saravanan, M. Maruthapandi, P. Das, J. H. Luong and A. Gedanken, *Nanomaterials*, 2021, **11**, 369.
55 T. Boobalan, M. Sethupathi, N. Sengottuvelan, P. Kumar, P. Balaji, B. Gulyás and A. Arun, *ACS Appl. Nano Mater.*, 2020, **3**, 5910–5919.
56 H. M. Chandra and S. Ramalingam, *Food Sci. Biotechnol.*, 2011, **20**, 15–21.
57 A. Sachdev and P. Gopinath, *Analyst*, 2015, **140**, 4260–4269.